JOURNAL OF MATERIALS SCIENCE 31 (1996) 2661–2665

The effect of Ti^{4+} ions on some magnetic properties of lithium ferrite

S. A. MAZEN*, A. H. WAFIK‡, S. F. MANSOUR*
*Physics Department, Faculty of Science, Zagazig University, Zagazig, Egypt and
‡Physics Department, Faculty of Science, Ain Shams University, 11566 Abbassia, Cairo, Egypt

Some magnetic properties of the spinel structure compound, $Li_{0.5+0.5x}Ti_xFe_{2.5-1.5x}O_4$, where $x = 0$–0.5, have been studied by different methods. The initial permeability, μ_i, was measured as a function of temperature at a constant frequency of 10 kHz. A maximum value was observed for each composition indicating the Curie temperature, T_c, which decreases with increasing titanium concentration. The magnetization, M, and the B–H loop were measured at RT in the range of magnetizing field from 0–1200 A m^{-1} and at constant field $H = 205$ A m^{-1}, respectively. The relative permeability, μ_r, depends on the magnetizing field and composition. It was found from the B–H loop that the remanence induction, B_r, and the apparent loss energy, P_S, depend on the composition but the coercive force, H_c, is independent of composition.

1. Introduction

It has been reported that the substitution of Ti^{4+} in ferrites has some remarkable influence on the magnetic and electric properties, e.g. controlling the anisotropy constant [1], affecting the permeability at room temperature [2] and exerting a great influence on the discontinuous magnetization [3]. Galt and co-workers [4, 5] found the initial permeability, μ_i, to be about 80 and 15 in sintered samples. Such low values in polycrystalline materials suggest that domain-wall movements are hindered and are not related to domain rotations. High-field magnetization measurements and Mössbauer effect measurements with and without an applied field have been performed on $Li_{1.125}Ti_{1.25}Fe_{0.625}O_4$ spinels [6].

Our previous work, recently published [3], has studied the composition dependence of discontinuous magnetization in Li–Ti ferrites. The present work is a continuation of the investigation of the effect of non-magnetic ions (Ti^{4+}) on some other magnetic properties of lithium.

2. Experimental procedure

Samples of $Li_{0.5+0.5x}Ti_xFe_{2.5-1.5x}O_4$ (where $x = 0, 0.1, 0.2, 0.3, 0.4$ and 0.5) were prepared using a standard ceramic method. X-ray diffraction and Mössbauer analysis were carried out [7] and showed that all samples were single-phase spinel. The samples were prepared in the form of toroids with an external diameter, r_o, of 8.2 mm, internal diameter, r_i, of 4.85 mm, and a height of about 0.55 mm.

2.1. The initial permeability and magnetization

The measurements of initial permeability, μ_i, and magnetization, M, (A m^{-1}) were based on Faraday's law of electromagnetic induction. The toroidal sample was used as a transformer core, the number of turns of primary and secondary coils, n_p and n_s, were 14 and 9, respectively. The circuit used is shown in Fig. 1.

The initial permeability, μ_i, was measured as a function of temperature at constant frequency $f = 10$ kHz of a sinusoidal wave and low magnetizing current $i_p = 20$ mA. The corresponding magnetizing field, H, was 14 A m^{-1}. The initial permeability, μ_i, is related to the induced voltage, V_s (V), in the secondary coil according to Poltinnikov and Turkerich [8], as

$$V_s = K\mu_i \quad (1)$$

where the constant K depends on f, n_p, n_s, i_p and geometrical dimensions of the toroidal samples

The magnetization, M, was measured at room temperature (RT) in the range of magnetizing current from 0–3.8 A, at constant magnetizing frequency $f = 50$ Hz. The corresponding magnetic field, H, was in the range of 0–1200 A m^{-1}. The magnetization, M, was calculated from the relation

$$M = \frac{B}{\mu} - H \quad (2)$$

where the magnetic flux density, B (T) was calculated according to Boll [9], as

$$B = \frac{50}{f}\left(\frac{50\,V_s}{10^4\,n_s A}\right) \quad (3)$$

0022–2461

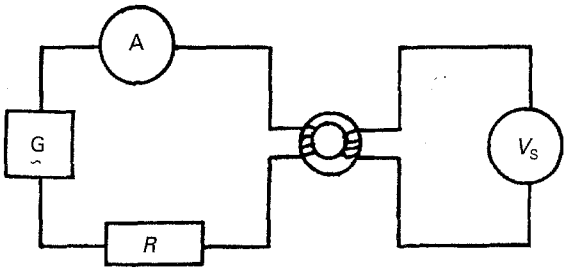

Figure 1 Measuring circuit for initial permeability and magnetization.

where A is the cross-sectional area (m^2) of the toroidal sample.

2.2. The B–H loop measurements

A loop tracer circuit was used to measure the coercive force, H_c, and the remanence induction, B_r, of the present samples. All the loops were measured at constant frequency ($f = 50$ Hz) and constant magnetizing current 0.6 A ($H = 205\ A\,m^{-1}$). The measurements were carried out on a CRO screen which was properly calibrated.

3. Results and discussion

3.1. The initial permeability

The thermal variation of initial permeability, μ_i, was recorded to determine the Curie temperature, T_c, for the above mentioned composition. Fig. 2 shows the change of μ_i with T(K). It is generally found that the curves are typical of multidomain grains showing a maximum in μ_i just below T_c.

Fig. 3a shows the variation of μ_i at RT versus titanium content while Fig. 3b shows the variation of porosity. It can be seen that with increasing titanium content, μ_i decreases and porosity increases. Fig. 3c shows the variation of T_c with titanium content. These results are given in Table I. It can be seen that T_c decreases with the increase of diamagnetic substitution Ti^{4+} and Li^{1+}. According to Mössbauer data [7] and White and Patton [10], the cation distribution can be taken as

$$(Li^{1+}_{0.5x}Fe^{3+}_{1-0.5x})^{A}[Li^{1+}_{0.5}Ti^{4+}_{x}Fe^{3+}_{1.5-x}]^{B}O^{2-}_{4}$$

(Formula I)

where titanium is localized on octahedral sites (B-sites) and lithium ions in excess of 0.5 move into tetrahedral sites (A-sites). Such a distribution will cause a decrease in A–B magnetic interaction [11] and thereby a decrease in the Curie point.

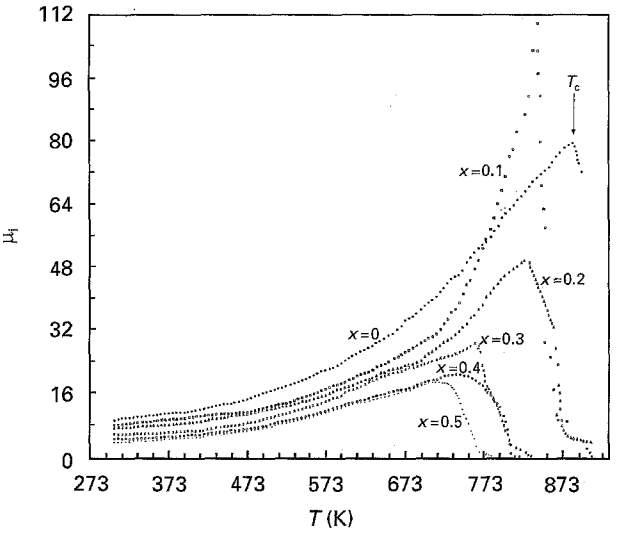

Figure 2 The initial permeability, μ_i, versus temperature, for the values of x indicated.

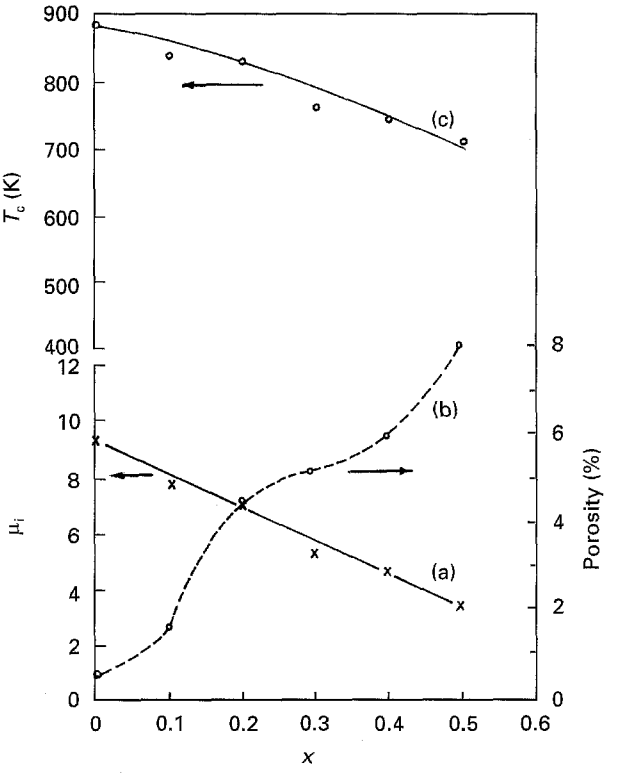

Figure 3 Dependence of (a) μ_i, (b) porosity, at RT, and (c) Curie temperature, T_c on titanium content.

3.2. Magnetization and relative permeability

The relationship between the magnetization, M, and magnetic field intensity, H, of the above-mentioned

TABLE I The values of Curie temperature, T_c, coercive force, H_c, remanence induction, B_r, and the apparent loss energy, P_s

x	$T_c(\pm 5\ K)$	$H_c(A\,m^{-1})$	$B_r(10^{-2}\ T)$	$P_s(10^{-4}\ W)$
0.0	888	159	10.3	1.9
0.1	843	157	9.9	1.8
0.2	828	154	7.2	1.0
0.3	763	157	5.8	0.8
0.4	743	155	4.1	0.3
0.5	709	156	2.2	0.2

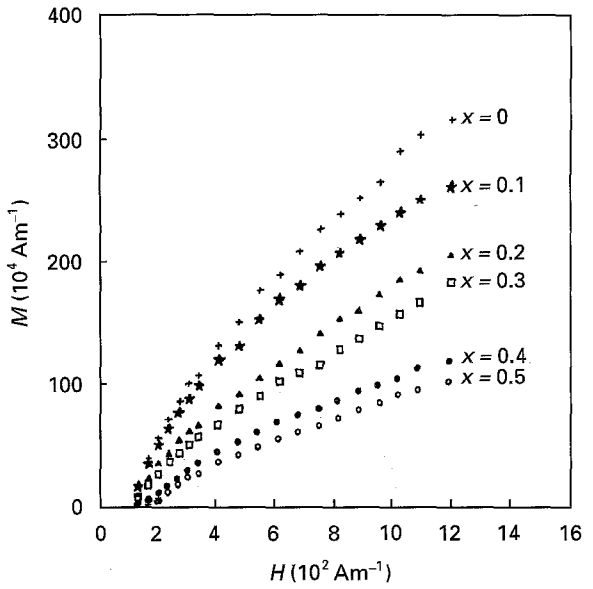

Figure 4 The relationship between magnetization, M, and magnetic field intensity, H at RT, for the values of x indicated.

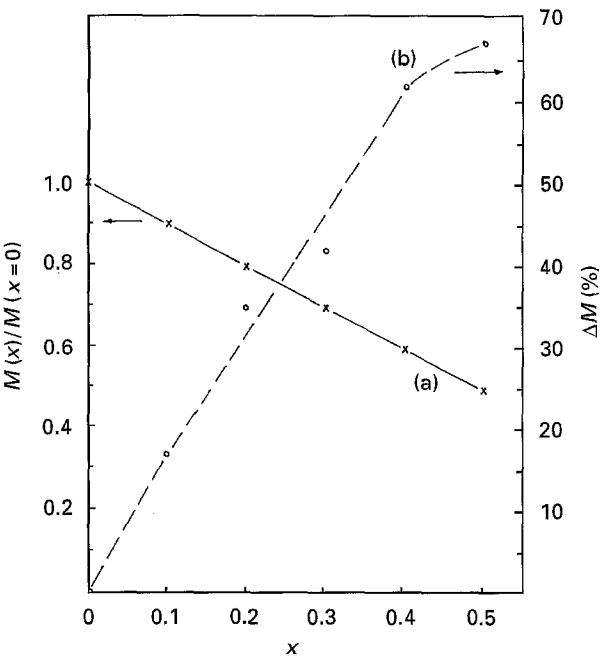

Figure 5 Dependence of (a) relative magnetization $M(x)/M(x = 0)$ and (b) its relative change, ΔM, on titanium content.

composition was studied at room temperature, 298 K. These results are shown in Fig. 4. It can be seen that for each composition, M increases with increasing H. In the present range of the magnetizing field ($H = 0$–$1200\ \mathrm{A\,m^{-1}}$), M does not show a saturation. The sample with $x = 0$ ($Li_{0.5}Fe_{2.5}O_4$) has the highest magnetization value (highest magnetic moment). Then M decreases with increasing titanium content. The decrease of M with increasing titanium content can be explained by Néel's theorem of ferrimagnetism [12]. The individual magnetization, M_A and M_B, of the two sublattices cannot be observed but instead the net magnetization has been measured. Because the two magnetizations are oppositely directed, then $|M| = |M_B| - |M_A|$. According to Joshi and Kulkarni [13], the net magnetic moment is given by

$$\mu_m(x) = \frac{H_B(x)}{H_B(x=0)}\mu_B - \frac{H_A(x)}{H_A(x=0)}\mu_A \qquad (4)$$

where μ_A and μ_B are the calculated magnetic moments in units of Bohr magneton for sites A and B, respectively. $H_A(x)$ and $H_B(x)$ are the magnitudes of the average magnetic fields for the A and B sites, respectively, where the ionic magnetic moments of Li^{+1} and Ti^{+4} are zero. It is assumed that the relative magnetization $M(x)/M(x = 0)$ at room temperature is proportional to $\mu_m(x)/\mu_m(x = 0)$. The values of relative magnetization $M(x)/M(x = 0)$ as a function of x were determined from Equation 4 where the values of hyperfine fields and distribution of Fe^{3+} ions on A and B sites at RT were taken from Mössbauer data [7]. These results are represented by curve (a) in Fig. 5. The percentage of the relative change in the magnetization, ΔM, at $H = 1200\ \mathrm{A\,m^{-1}}$ is given by

$$\Delta M = \left[1 - \frac{M(x)}{M(x=0)}\right] \times 100 \qquad (5)$$

The dependence of ΔM against x is depicted in curve (b) of Fig. 5. It can be seen that the relative magnetization decreases with increasing titanium concentration. Thus the variation of magnetic moment with titanium content could be explained by assuming that, as the concentration of titanium ions increases, the relative number of ferric ions decreases on both A and B sites, but more on the B sites than the A sites. This will cause the A–B interaction to be reduced. According to Néel's molecular field model, the A–B exchange interactions are stronger than those of A–A or B–B. In the ionic distribution, Ti^{4+} does not participate in the exchange interaction Fe_A^{3+}–O–Fe_B^{3+} causing a decrease in the magnetization. The decrease in A–B interaction was suggested also to be due to the decrease which was observed in the Curie temperature, as shown in Fig. 3c.

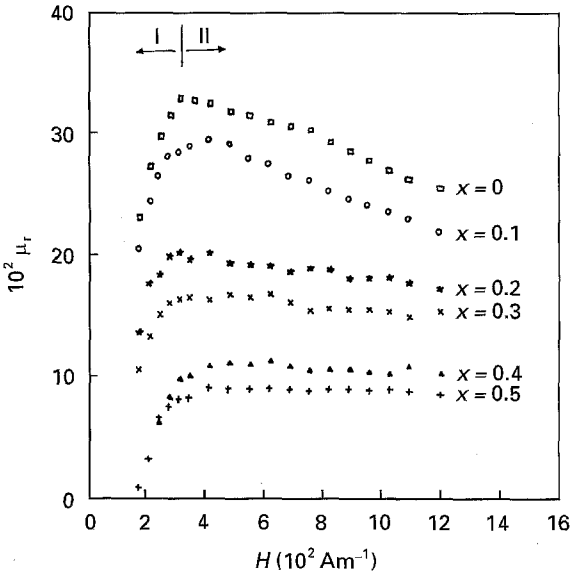

Figure 6 Relative permeability, μ_r, as a function of the magnetizing field, H.

Fig. 6 shows the relative permeability, $\mu_r (= B/\mu_0 H)$ with the magnetizing field, H. The behaviour of μ_r

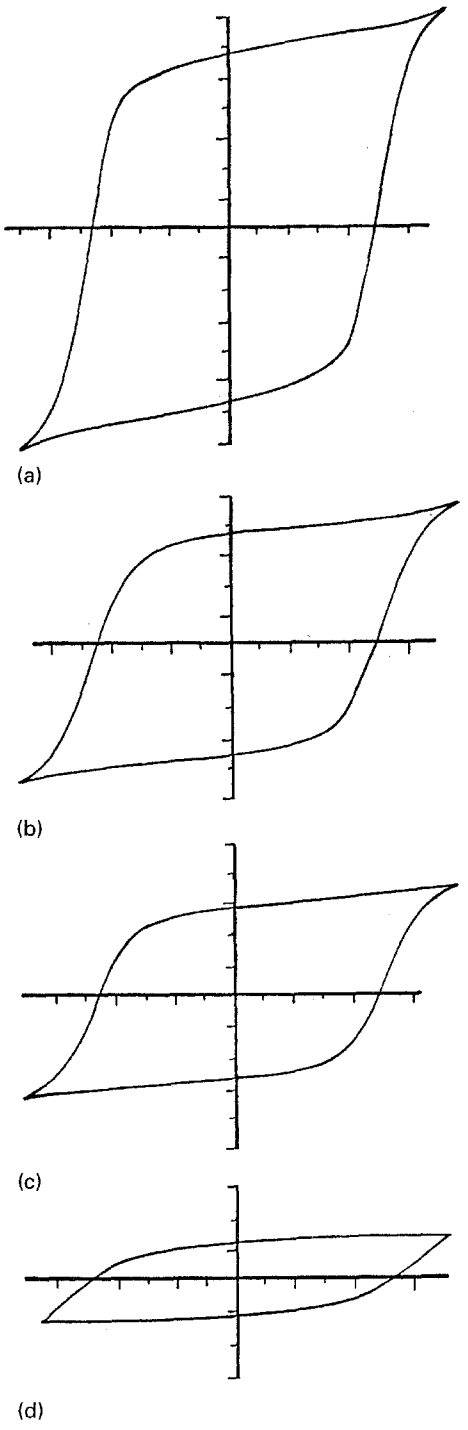

Figure 7 The B–H loops at a constant frequency of 50 Hz and constant magnetizing current of 0.6 A (i.e. $H = 205\ \mathrm{A\,m^{-1}}$) for (a) $x = 0$, (b) 0.2, (c) 0.3 and (d) 0.5.

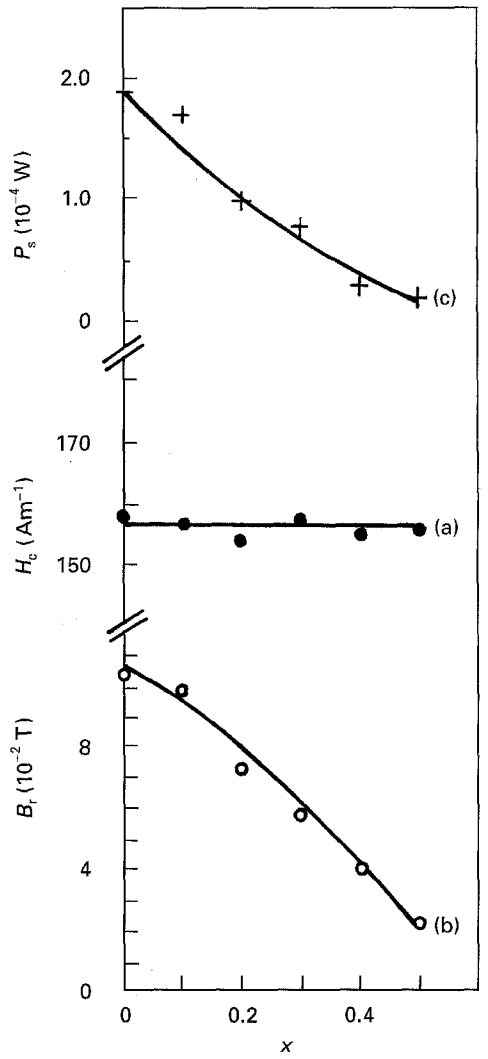

Figure 8 Dependence of (a) coercive force, H_c, (b) the remanence induction B_r and (c) the apparent loss energy, P_s, on titanium content.

versus H could be divided into two stages (stages I and II are shown in the figure). In stage I, the increase of the magnetizing field causes a pronounced increase of μ_r until it reaches a maximum value. The increment of μ_r decreases with increasing non-magnetic ions (i.e. titanium and lithium). The increment of μ_r in stage I could be related to the aligning effect of the applied field on the ionic spins, in such a way that the increase of H causes very rapid increases in flux density, B, causing pronounced increase of μ_r. The maximum value of μ_r for all investigated samples takes place in the range of applied magnetizing field from $H \approx 3.0$–$3.7\ \mathrm{A\,m^{-1}}$. Generally, μ_r decreases with increasing titanium concentration.

In stage II, for samples with $x = 0$ and 0.1, μ_r decreases with increasing H. The decrease of μ_r for these two samples is more pronounced relative to the other samples examined. The samples with $x = 0.2$ and 0.3 show slight decrease of μ_r, while samples with $x = 0.4$ and 0.5 show nearly constant values of μ_r with increasing H. The behaviour of μ_r versus H in stage II could be interpreted as follows: samples with $x = 0$ and 0.1 have the highest spin ordering (highest intrinsic magnetization) relative to the other samples. This means that the ionic ordering of these two samples is closer to the saturation state than the others. Accordingly, the increase of H in stage II could cause a slight increase of B giving rise to a distinct decrease in μ_r. The aligning effect of the field would continue, but with a smaller increase of B than in stage I because the ionic ordering of the samples with $x \geq 0.2$ would be further from the saturation state than the samples with $x < 0.2$, the action of the aligning effect of the field would be more pronounced on the samples with $x < 0.2$. Thus the produced flux density would be greater for $x \geq 0.2$, in such a way that $\mathrm{d}B/\mathrm{d}H$ decreases very slightly for $x = 0.2$ and 0.3 or even stays nearly constant for $x = 0.4$ and 0.5.

3.3. Coercive force and remanence induction

The B–H loops were measured for the above-mentioned samples at a constant frequency of 50 Hz and constant magnetizing current of 0.6 A (i.e. $H = 205\ \mathrm{A\,m^{-1}}$). These loops are schematically represented in Fig. 7. Fig. 8a and b show both the coercive force H_c ($\mathrm{A\,m^{-1}}$) and the remanence induction B_r (T) as a function of composition. These values are given in Table I. It is clear that H_c is almost independent of titanium concentration. The highest values of B_r were found for $x = 0$ and 0.1, the samples of highest intrinsic magnetization. Then B_r decreases with increasing titanium content indicating the decrease of intrinsic magnetization.

Fig. 8c shows the behaviour of the apparent energy loss P_s(W) versus composition, where P_s is calculated according to Boll [9], as

$$P_s = 10^2 m \frac{f}{50}\left(\frac{B}{45}\right)\frac{H_{\mathrm{eff}}}{\gamma} \qquad (6)$$

where m is the mass (kg) of toroidal samples, $f = 50$ Hz, B is the magnetic flux density (T), H_{eff} is the effective value of the magnetizing field H ($\mathrm{A\,m^{-1}}$), and γ is the density ($\mathrm{kg\,m^{-3}}$). It is clear from Fig. 8c that P_s decreases with increasing titanium content which indicates the decrease in the number of domain walls. The values of P_s are given in Table I.

4. Conclusions

1. According to Neel's molecular field model, we suggest that the decrease in A–B interaction is due to the decrease in magnetization and Curie temperature.

2. Two stages in the behaviour of μ_r were discerned, according to the aligning effect of the applied field on the ionic spins.

References

1. T. G. W. STIJNTIES, J. KLERK and A. BROESE VAN GROENOU, *Philips Res. Rep.* **25** (1970) 95.
2. R. HOHNE, K. MELZER, H. HOCHSCHILD, G. LIBOR and R. KRAUSE, *Phys. Status solids (a)* **27** (1975) K 711.
3. A. H. WAFIK, S. A. MAZEN and S. F. MANSOUR, *J. Phys. D Appl. Phys.* **26** (1993) 2010.
4. J. K. GALT, I. J. MATTHIAS and J. P. REMEIKA, *Phys. Rev.* **79** (1950) 391.
5. J. K. GALT, *ibid.* **85** (1952) 664.
6. J. L. DORMANN, M. EL HARFAOUI, M. NOGUES and J. JOVE, *J. Phys. C Solid State Phys.* **20** (1987) L 161.
7. A. A. YOUSIF, M. E. ELZAIN, S. A. MAZEN, H. H. SUTHERLAND, M. H. ABDALLA and S. F. MANSOUR, *J. Phys. C Condensed Matter* **6** (1994) 5717.
8. S. A. POLTINNIKOV and E. I. TURKEVICH, *Sov. Phys. Solid State* **8** (1966) 1144.
9. R. BOLL, "Weichmagnetische Werkstoffe", Vol 3, 'Völlig überarbeitete und erweiterte Auflage", (Vacuumschmelze GMBH, 1977).
10. G. O. WHITE and C. E. PATTON, *J. Magn Magn Mater.* **9** (1978) 299.
11. Y. YAFET and C. KITTEL, *Phys. Rev.* **87** (1952) 290.
12. K. STANDLY, "Oxide Magnetic Materials" (Clarendon, Oxford, 1972).
13. H. H. JOSHI and R. G. KULKARNI, *J. Mater. Sci.* **21** (1986) 2138.

Received 12 January
and accepted 20 November 1995